

Effect of *tert*-butyl substitution on controlling the orientation of TADF emitters in guest–host systems†

Prakhar Sahay,^a Ettore Crovini,^b Kleitos Stavrou,^c Zhen Zhang,^d Binh Minh Nguyễn,^a Daniel Wagner,^e Peter Strohriegl,^e Stefan Bräse,^{df} Andrew Monkman,^{id}^c Eli Zysman-Colman^{id}^{*b} and Wolfgang Brütting^{id}^{*a}

Organic light-emitting diodes (OLEDs) using thermally activated delayed fluorescence (TADF) materials as emitters have been reported to achieve 100% internal quantum efficiency due to their ability to harvest both singlet and triplet excitons. This is due to the small singlet–triplet energy gap in the emitter material that allows reverse intersystem crossing of excitons formed in the non-emissive triplet state to be endothermally upconverted to the emissive singlet state. Compared to phosphorescent molecules, the less bulky TADF molecules show a stronger tendency for horizontal alignment in vacuum-deposited films, which leads to an enhancement of the light-outcoupling from the OLED. In this work, we compare how changes in the structure of a linear acceptor–donor–acceptor indolocarbazole–triazine TADF emitter with *tert*-butyl groups affect molecular alignment across a range of different host matrices. We discuss the effects of their molecular electrostatic potentials and inertial moments as well as the glass transition temperatures of the host matrices. We observe that our previously reported molecule ICzTRZ with *tert*-butyl substitution on the distal phenyl rings of the acceptor yields the strongest horizontal alignment and, accordingly, the highest external quantum efficiency in OLEDs. By contrast, the absence of *tert*-butyl groups within the emitter leads to significantly lower alignment.

Introduction

In organic light-emitting diodes (OLEDs), thermally activated delayed fluorescent (TADF) emitters are able to harvest both singlet and triplet excitons. This is made possible by a reverse intersystem crossing (RISC) process that offers a route to the upconversion of excitons from the non-emissive triplet state to the emissive singlet state, ultimately leading to up to unity internal quantum efficiency (IQE) in the device, compared to

the use of conventional fluorescent emitters where IQE is limited to 25%.

One of the first examples of this phenomenon was reported by Adachi and co-workers in 2012 for the TADF emitter 4CzIPN, where the device showed an IQE of 93% and a maximum external quantum efficiency (EQE_{max}) of 19.3%.¹ RISC is mediated by a three-state vibronic coupling-assisted spin–orbit coupling mechanism involving two different triplet states which must be close in energy. This implies that RISC is highly dependent on the host matrix used to embed the emitter.^{2,3} It is also important to choose a suitable host matrix to avoid luminescence quenching due to aggregation of the emitter.⁴ Efficient TADF molecules need to have a low energy splitting (<200 meV) between the emissive charge transfer state with singlet character (¹CT), the triplet CT state (³CT) and the localized exciton triplet state (³LE). LE states refer to a local excitation confined at a specific region on the molecule, *i.e.* either the donor or acceptor part, whereas CT states are extended over the whole molecule because they are associated with the transfer of charge between them. The magnitude of the singlet–triplet gap ΔE_{ST} is proportional to the exchange integral of the orbitals describing the transitions to the lowest energy singlet and triplet states. Thus, ΔE_{ST} becomes smaller as the

^a Experimental Physics IV, Institute of Physics, University of Augsburg, Augsburg, Germany. E-mail: wolfgang.brueetting@uni-a.de

^b Organic Semiconductor Centre, EaStCHEM School of Chemistry, University of St Andrews, St Andrews, UK. E-mail: eli.zysman-colman@st-andrews.ac.uk

^c Department of Physics, Durham University, Stockton Road, Durham, UK

^d Institute of Organic Chemistry, Karlsruhe Institute of Technology, Karlsruhe, Germany

^e Macromolecular Chemistry, University of Bayreuth, Bayreuth, Germany

^f Institute of Biological and Chemical Systems – Functional Molecular Systems, Karlsruhe Institute of Technology, Eggenstein-Leopoldshafen, Germany

† Electronic supplementary information (ESI) available: Synthesis protocols, computational data obtained from DFT and TD-DFT, thermal analysis, molecular geometry (thickness & aspect ratio) studies, orientation measurements in different hosts, and additional OLED device data including light outcoupling simulations. See DOI: <https://doi.org/10.1039/d4tc01195c>

wave function overlap between the highest occupied molecular orbital (HOMO) and lowest unoccupied molecular orbital (LUMO) of the molecule decreases, a feature that is generally observed in highly twisted donor-acceptor type molecules.⁵ Another common strategy to minimize ΔE_{ST} is to incorporate an aromatic spacer bridging moiety between the donor and acceptor groups to further electronically isolate the electron and hole of the intramolecular CT state.⁶

TADF emitters often present highly anisotropic molecular structures, which offers an advantage in terms of preferential (horizontal) alignment of the optical transition dipole moments (TDMs), thus enhancing the EQE of TADF OLEDs. Randomly or specifically, vertically oriented emitter molecules dissipate a significant portion of their energy into trapped optical modes, for example, waveguided or surface plasmon modes, thus decreasing the light outcoupling and EQE of the OLED. An orientation parameter θ is used to quantify the alignment of molecular TDMs.⁷ It is defined as the second moment of the orientation distribution $\langle \cos^2\vartheta \rangle$, where ϑ is the angle between the substrate normal and the TDM vector on the molecule. θ can also be understood as the fraction of optical power emitted by vertical TDM components in relation to all TDMs in an ensemble of molecules. The goal is to align TDMs horizontally, *i.e.*, parallel to the substrate, thus minimizing θ .

As mentioned above, molecular shape plays a crucial role in governing the orientation parameter of a film. The tendency to form optically anisotropic films is enhanced with disc- or rod-like structures,⁸ though the exact definition of these terms is hard to quantify. For neat films, molecular alignment can be probed by variable angle spectroscopic ellipsometry (VASE),⁸ whereas in light-emitting guest-host systems angular dependent photoluminescence (ADPL) is the method of choice, which involves exciting the films using a laser and studying the emitted optical radiation pattern.⁹ Please note that optical anisotropy (as determined by VASE) and emitter orientation (probed by ADPL) are related to distinct molecular properties, *i.e.* molecular polarizability in the former case and TDM vector alignment in the latter case.¹⁰ However, specifically for rod-shaped molecules, the TDM vector and the largest component of the polarizability tensor are typically collinear and point along the long axis of the molecule. Thus, in such cases,

molecular orientation and TDM alignment can be used (more or less) synonymously.

Controlling emitter orientation in vapor-deposited films has been linked to the field of glass physics, where it has been demonstrated that the ratio between the substrate temperature (T_s), on which the film is grown, and the glass transition temperature (T_g) of the organic material allows controlling their emitting TDM orientation.¹¹ This correlation has been studied extensively in our previous work where we established that with a higher host T_g , the emitter molecules tend to align more horizontally on the surface of the substrate due to the reduced diffusivity of molecules, resulting in less time for them to equilibrate towards random or even vertical orientation.^{12,13}

Recent studies of linear-shaped organic molecules, such as **BSB-Cz**, have been established to be more than 90% horizontally oriented.¹⁴ Indolocarbazole (ICz) based emitters have likewise been shown to be highly horizontally aligned, where the ICz group acts as a weak, planar, and rigid donor. The use of ICz-containing emitters has led to devices showing high EQE_{max} (Fig. 1).¹⁵ For instance, Xiang *et al.* reported the emitter **IndCzpTR1** that has a Φ_{PL} of 75.2% and a delayed fluorescence (DF) lifetime, τ_d , of 25.48 μ s along with a θ factor of 0.27 in neat film. A related, rather horizontally oriented variant **IndCzpTR2** has also been reported with a Φ_{PL} of 71.9% and a τ_d of 34.41 μ s with a θ factor of 0.16 in neat film.¹⁶ We previously reported the emitter **ICzTRZ**, which exhibits highly horizontal orientation of its TDM in multiple host matrices (mCP: $\theta = 0.12$, mCBP: $\theta = 0.09$, DPEPO: $\theta = 0.06$) and has a Φ_{PL} of 70% and a τ_d of 121.1 μ s.¹⁵ Indeed, **ICzTRZ**, with its symmetric acceptor-donor-acceptor structure containing distal *tert*-butyl substituents, is among the most horizontally aligned TADF emitters known so far.¹⁷

In this work, we investigate the impact of the position of the *tert*-butyl (^tBu) substituents on the TDM alignment of the emitter (Fig. 2). We find that the placement of the ^tBu groups on the two triazine acceptors in **ICzTRZ** leads to the most strongly horizontal alignment of the TDMs of the four derivatives, while the unsubstituted analogue, **ICzTRZ-0**, has a much less horizontal orientation of its TDMs. We discuss our observations with respect to the electronic structure of the emitter molecules and their geometries as well as the glass transition

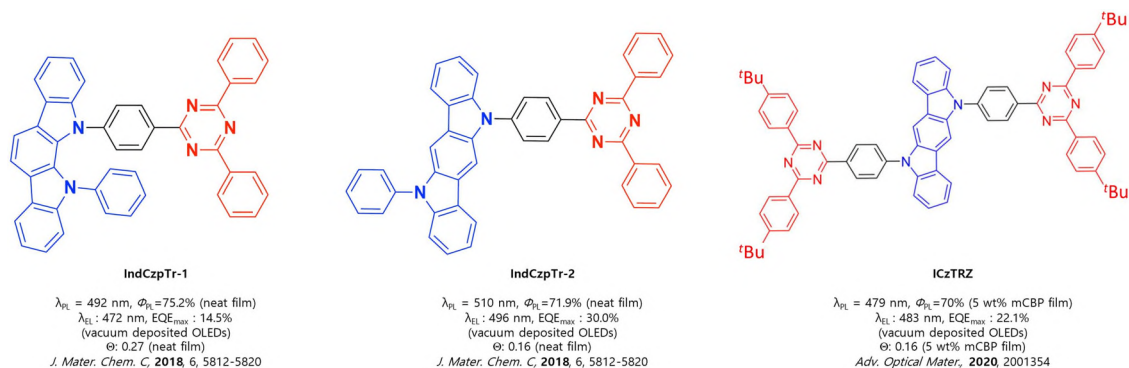


Fig. 1 Chemical structures and performance of known indolocarbazole based TADF emitters.

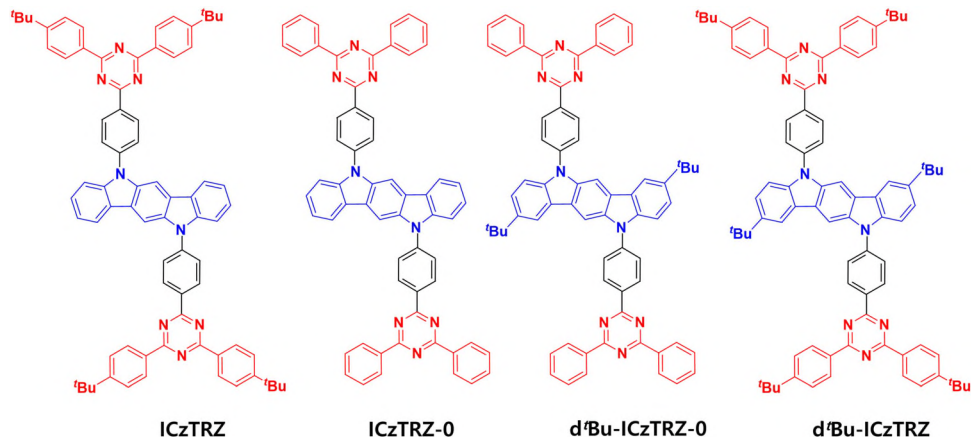


Fig. 2 Molecular structures of the ICzTRZ series of emitters under consideration.

temperatures of the host materials and compare their performance in OLEDs. Details of the synthesis and characterization of the emitters are given in ESI.†

Results and discussion

Density functional theory calculations

Density functional theory (DFT) and time-dependent DFT (TD-DFT) calculations in the gas phase at the PBE0/6-31G(d,p) level were used to explore how the reported structural modifications to the previously reported ICzTRZ would impact its frontier molecular orbitals (FMOs), energy levels, and excited-state properties (Fig. 3). Their corresponding energies were obtained using the Tamm–Dancoff approximation¹⁸ to TD-DFT (TDA-DFT) at the same level of theory. All calculations were conducted in the gas phase.

The highest occupied molecular orbital (HOMO) and lowest unoccupied molecular orbital (LUMO) energies of ICzTRZ were calculated as -5.19 and -1.75 eV, respectively.¹⁵ ICzTRZ-0 shows a slight weakening (strengthening) of the donor (acceptor) character of the molecule, which was expected due to the absence of the electron-donating *tert*-butyl groups attached to the triazine acceptor, which is conjugated to the indolocarbazole donor, with HOMO and LUMO levels of -5.25 eV and -1.86 eV. The insertion of the electron-donating *tert*-butyl groups on the indolocarbazole in d⁴Bu-ICzTRZ-0 leads to a modestly destabilized HOMO level of -5.15 eV compared to ICzTRZ, while the LUMO level is nearly identical to that of ICzTRZ-0 at -1.84 eV since the acceptor moiety is the same. The presence of *tert*-butyl groups on both the donor and acceptor in d⁴Bu-ICzTRZ results in the most destabilized HOMO level of -5.09 eV, and an electron-accepting character that closely resembles that of ICzTRZ, with a

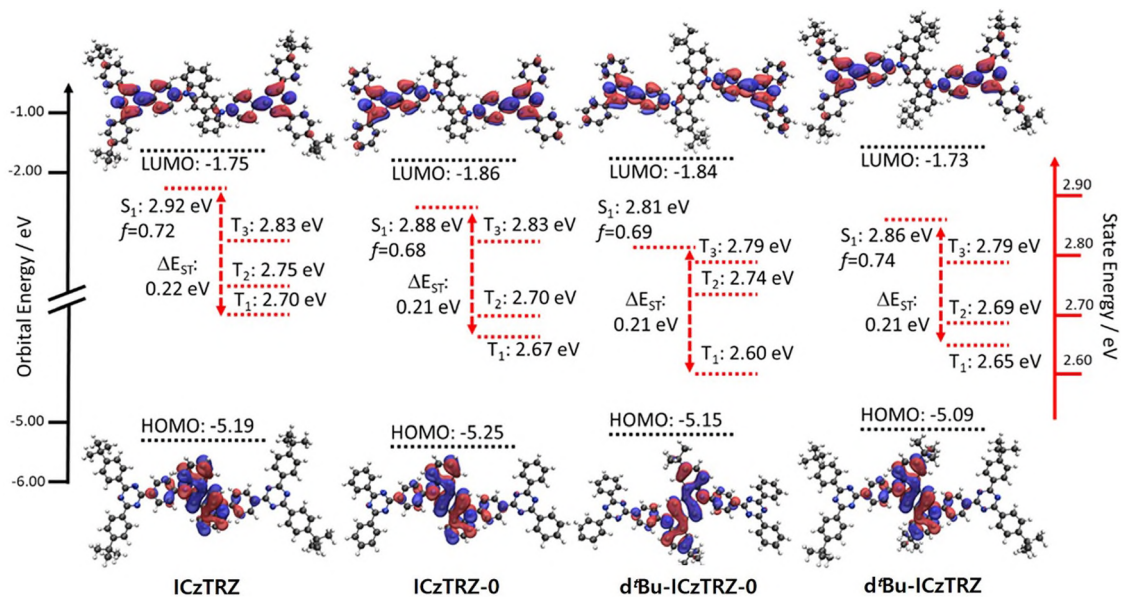


Fig. 3 HOMO, LUMO and excited states energies of ICzTRZ, ICzTRZ-0, d⁴Bu-ICzTRZ-0, and d⁴Bu-ICzTRZ (obtained via DFT and TD-DFT at the PBE0/6-31G(d,p) level, isovalues: MO = 0.02, density = 0.0004).

Table 1 Summarizing the HOMO, LUMO and excited-state energies for all four emitter materials

Material	HOMO/eV	LUMO/eV	S ₁ energy (¹ CT)/eV	T ₁ energy (³ CT)/eV	ΔE _{ST} /eV
ICzTRZ	-5.19	-1.75	2.92	2.70	0.22
ICzTRZ-0	-5.25	-1.86	2.88	2.67	0.21
d ^t Bu-ICzTRZ-0	-5.15	-1.84	2.81	2.60	0.21
d ^t Bu-ICzTRZ	-5.09	-1.73	2.86	2.65	0.21

LUMO level of -1.73 eV. Fig. 3 and Table 1 summarize the HOMO and LUMO levels for the four emitter molecules. Details of the calculations as well as other relevant orbitals can be found in ESI† (Fig. S3–S6 and Tables S1–S4).

All materials exhibit a very similar excited-state landscape, with almost identical ΔE_{ST} values (between the lowest lying singlet and triplet state) of 0.22 eV for ICzTRZ, and 0.21 eV for each of ICzTRZ-0, d^tBu-ICzTRZ-0 and d^tBu-ICzTRZ. In total, there are three energetically close-lying triplet states (see Tables S1–S4 in the ESI†). The lowest two, T₁ and T₂, possess CT character, similar to that of S₁, and so spin-orbit coupling (SOC) between these states is expected to be small. T₃ possesses LE character (localized on the ICz donor) and so SOC between this state and S₁ will be strongest and RISC is likely to proceed with the involvement of this LE triplet state.^{19–23} Note, however, that even two triplet states with the same character, e.g. two CT triplets with different orbital configurations, are sufficient for RISC to proceed efficiently, as has been shown recently.²⁴ The transition from S₀ to the S₁ state in all four compounds has high oscillator strength (*f*), with values of 0.72, 0.68, 0.69, and 0.74 for ICzTRZ, ICzTRZ-0, d^tBu-ICzTRZ-0, and d^tBu-ICzTRZ, respectively. Comparing ICzTRZ to ICzTRZ-0, we can see that the removal of the *tert*-butyl groups stabilizes the excited states, with S₁ and T₁ energies changing from 2.92 and 2.70 eV to 2.88 and 2.67 eV, respectively. The presence of the *tert*-butyl groups on the donor in d^tBu-ICzTRZ-0, correlates with a stabilization of the excited states to 2.81 eV for S₁ and 2.60 eV for T₁. With six *tert*-butyl groups, d^tBu-ICzTRZ has only slightly destabilized excited states compared to d^tBu-ICzTRZ-0, S₁ and T₁ levels of 2.86 and 2.65 eV, respectively.

Electrostatic surface potential (ESP) & inertial moments

In addition to the above discussed excited-state properties, we also calculated the electrostatic surface potential (ESP) of the molecules in the ground state (Fig. 4). To this end, the

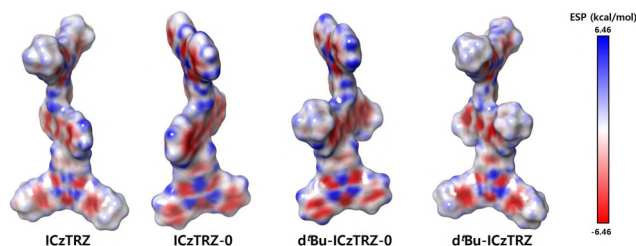


Fig. 4 Electrostatic surface potential (ESP) maps extracted from DFT calculation for the emitter series.

molecular structures of ICzTRZ-0, ICzTRZ, d^tBu-ICzTRZ-0 and d^tBu-ICzTRZ were optimized using the Jaguar software from Schrödinger.²⁵ Please note that due to their high flexibility, all four emitter molecules have many conformers that are close in energy and deviate only slightly in their dihedral angles, as was shown by Stavrou *et al.*²⁶ However, they are qualitatively very similar. We also want to emphasize that the ground state geometries of the four emitters obtained from the Schrödinger software are in excellent agreement with the results from Gaussian shown in Fig. 3; this is particularly valid for the dihedral angles between the indolocarbazole donor core and the two triazine acceptor units.

As evident from Fig. 4, the planar ICz donor unit and the two (also close to planar) TRZ acceptor units are strongly twisted with respect to each other. Specifically, the dihedral angles between the TRZ acceptor and the ICz donor are about 50° in all four emitters. Note that the phenyl linker between the ICz core and the TRZ unit is actually almost coplanar with the latter (twist angle of 1–3° only) whereas it has a twist angle of 47–48° to the ICz unit.

The unsubstituted ICz cores of ICzTRZ and ICzTRZ-0 have a pronounced negative ESP, whereas the unsubstituted TRZ units of ICzTRZ-0 and d^tBu-ICzTRZ-0 have a more mixed character of positive and negative ESP regions being close by. Adding the *tert*-butyl substituents to either of these groups seems to induce a certain degree of shielding of the ESP of the emitter skeleton proximal to these groups. It has been shown in the literature that the ESP landscape of an emitter can influence its orientation in vacuum-deposited guest-host systems,²⁷ as will be discussed further below.

Furthermore, the addition or removal of *tert*-butyl groups changes the overall mass and the mass distribution of the molecule. To quantitatively analyse these effects, we extracted the principal moments of inertia of the four emitters at their respective optimized geometries, represented as I₁, I₂ and I₃ (Table 2). The corresponding eigenvectors are given in Fig. S13 of the ESI†

To begin with, molecular weight (see Table 3) increases from ICzTRZ-0 to d^tBu-ICzTRZ-0 and ICzTRZ and reaches a maximum value for d^tBu-ICzTRZ. However, regarding their aspect ratio, ICzTRZ-0 shows the highest value of 7.73, whereas d^tBu-ICzTRZ-0 and d^tBu-ICzTRZ, have the lowest aspect ratios of 4.76 and 4.53, respectively. The aspect ratio of 5.73 for ICzTRZ lies in between these other values. Further information concerning the geometric factors of these emitter molecules as well as the aspect ratio calculation for the host materials can be found in the ESI† (Table S7).

Table 2 Calculated inertial moments and aspect ratios of the ICzTRZ series of molecules

Molecule	I ₁ /amu Å ²	I ₂ /amu Å ²	I ₃ /amu Å ²	Aspect ratio $\frac{\sqrt{I_3 \cdot I_2}}{I_1}$
ICzTRZ	18 148	103 829	104 334	5.73
ICzTRZ-0	7917	60 165	62 215	7.73
d ^t BuICzTRZ-0	13 426	60 494	67 797	4.76
d ^t Bu-ICzTRZ	23 630	104 546	109 732	4.53

Table 3 T_g and M_w values for ICzTRZ series molecules and host materials

Molecule	$T_g/^\circ\text{C}$	Molecular weight/g mol ⁻¹
ICzTRZ	253	1095
ICzTRZ-0	NA	871
d ^t Bu-ICzTRZ-0	227	983
d ^t Bu-ICzTRZ	264	1208
mCP	65	409
mCBP	92	485
mCBP-CN	113	510
DPEPO	93	571

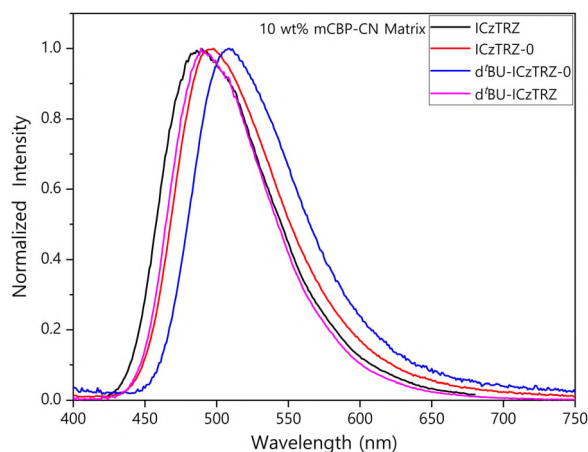
Glass transition temperature measurements

Next, given the reported importance of the glass transition temperature (T_g) as a factor controlling the orientation of the TDM, we also measured the T_g 's of the emitters (see ESI,† Fig. S7–S12). ICzTRZ, d^tBu-ICzTRZ-0, and d^tBu-ICzTRZ have T_g values of 253, 227, and 264 °C, respectively. Although no T_g could be determined for ICzTRZ-0, we expect it to be the lowest of all four emitters as the magnitude of the T_g roughly scales with molecular weight (Table 3). However, as the guest concentration is 10 wt% for the used guest–host films in this study, the T_g of the blend is expected to roughly mirror that of the host. The host T_g 's increase from mCP (65 °C) *via* mCBP (92 °C) and DPEPO (93 °C) to mCBP-CN (113 °C).

Photoluminescence spectra

The solid-state photophysics of the four emitters were studied at 10 wt% concentration guest–host films. This emitter concentration has been used in several of our orientation studies before, where no significant difference has been found between 5 and 10 wt% concentration.¹² As host we used mCBP-CN, which is a bipolar material with a sufficiently high triplet energy to ensure that excitons are confined on the emitters. The steady-state photoluminescence (PL) spectra are shown in Fig. 5.

ICzTRZ emits with a peak maximum at λ_{PL} of 490 nm, whereas ICzTRZ-0 emits at λ_{PL} at 496 nm. As discussed above, the absence of *tert*-butyl groups on the TRZ acceptor in ICzTRZ-0, compared to ICzTRZ enhances the acceptor strength, causing

**Fig. 5** Steady-state PL spectra of the four TADF emitters doped into an mCBP-CN host matrix at 10 wt% ($\lambda_{\text{exc}} = 365$ nm).**Table 4** Photophysical properties of ICzTRZ, ICzTRZ-0, d^tBu-ICzTRZ-0 and d^tBu-ICzTRZ at 10 wt% concentration in mCBP-CN host (extracted from Fig. 5 and 6)

	ICzTRZ	ICzTRZ-0	d ^t Bu-ICzTRZ-0	d ^t Bu-ICzTRZ
$\lambda_{\text{PL}}/\text{nm}$	490	496	508	492
FWHM/meV	440	450	410	410
$A_{\text{PF avg.}}/\text{a.u.}$	0.76	0.71	0.82	0.74
$\tau_{\text{p avg.}}/\text{s}^a$	9.47×10^{-9}	1.00×10^{-8}	8.69×10^{-9}	8.25×10^{-9}
$A_{\text{DF avg.}}/\text{a.u.}$	2.23×10^{-5}	5.75×10^{-5}	6.41×10^{-5}	1.52×10^{-5}
$\tau_{\text{d avg.}}/\text{s}^a$	8.33×10^{-5}	6.13×10^{-5}	4.99×10^{-5}	1.31×10^{-4}
$k_{\text{F avg.}}/\text{s}^{-1}$	1.06×10^8	1.00×10^8	1.15×10^8	1.21×10^8
$k_{\text{ISC avg.}}/\text{s}^{-1}$	2.17×10^7	3.29×10^7	3.57×10^7	2.98×10^7
$k_{\text{RISC avg.}}/\text{s}^{-1}$	1.51×10^4	2.44×10^4	2.90×10^4	1.01×10^4

^a Average values were extracted from the averaging of the multiple exponentials used to fit the prompt and delayed lifetimes using the

following equation: $\tau_{\text{avg.}} = \frac{\sum_{i=1}^n (A_i \tau_i^2)}{\sum_{i=1}^n (A_i \tau_i)}$.

a bathochromic shift in the PL spectrum. d^tBu-ICzTRZ and d^tBu-ICzTRZ-0 have their λ_{PL} at 492 and 508 nm, respectively. For the first, the effect of the *tert*-butyl groups' presence on both the donor and acceptor units has complementary effects on their strengths, leading to an emission that is intermediate between ICzTRZ and ICzTRZ-0. However, d^tBu-ICzTRZ-0 has a significantly red shifted PL spectrum because of the *tert*-butyl groups' presence on the donor unit (indolocarbazole), enhancing only the donor strength. Interestingly, the overall PL full width at half maximum (FWHM) of d^tBu-ICzTRZ and d^tBu-ICzTRZ-0 films is at 410 meV (a factor mainly determined by the fluorescence decay of S₁ excitons to the sub-vibrational states of the S₀ state, the conformational dispersion, and the intermolecular interactions/aggregation). This value is smaller than those of ICzTRZ and ICzTRZ-0 which is at around 440 to 450 meV (Table 4). This is attributed to the presence of the *tert*-butyl groups on the donor unit which appear to minimize the intermolecular interactions that lead to aggregation effects, *i.e.*, broader PL spectrum.

Time-resolved photoluminescence decays

The time-resolved (TR) PL decays of the four emitters in mCBP-CN host (at 10 wt% emitter concentration in the film) are shown in Fig. 6. The TRPL decays of ICzTRZ-0 and d^tBu-ICzTRZ-0 have similar TADF contributions, as evidenced by the similar amplitude and lifetime of the delayed fluorescence (DF) regime. The TADF behavior of d^tBu-ICzTRZ and ICzTRZ is also very similar between the two molecules, although the contribution from their DF regime is slightly smaller than for the former two, indicating somewhat weaker RISC in their case.

The triplet energy of ICzTRZ was previously reported as 2.62 eV (at 5 wt% concentration in mCBP host),¹⁵ and is in good proximity with the lowest local triplet energy of the ICz donor unit.^{28–30} This means that although the lowest CT triplet level might change between the four molecules, the lowest energy LE triplet state, which is crucial in promoting RISC,^{2,3} will always be within the reported range. This partially explains why the absence of the *tert*-butyl groups on the TRZ acceptor units (in ICzTRZ-0 and d^tBu-ICzTRZ-0) leads to a stabilization of their S₁ energies and also to a smaller energy difference between ¹CT

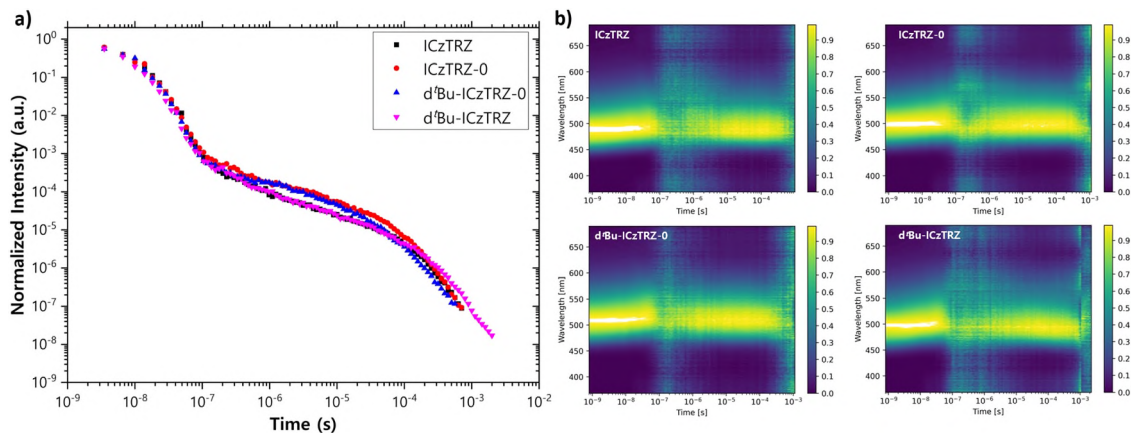


Fig. 6 Time-resolved PL (a) decays and (b) contour plots of **ICzTRZ**, **ICzTRZ-0**, **d⁴Bu-ICzTRZ-0** and **d⁴Bu-ICzTRZ** at 10 wt% concentration in mCBP-CN at room temperature under an excitation wavelength of 355 nm.

and ³LE compared to the two other emitters. This thus results in an improved triplet harvesting efficiency (higher amplitude of the DF regime in Fig. 6) in the latter two emitters.

The time-resolved decay kinetics were calculated according to the method of Dias *et al.*⁵ and are shown in Table 4. The prompt fluorescence (PF) lifetime, τ_p , is comparable across all four emitters, while the average delayed fluorescence (DF) lifetime, τ_d , adheres to the following trend: the emitters with unshielded triazine units (**ICzTRZ-0** and **d⁴Bu-ICzTRZ-0**) have shorter τ_d of around 50 μ s, while the other two emitters have a τ_d closer to 100 μ s. The corresponding k_{RISC} values are 1.51×10^4 , 2.44×10^4 , 2.90×10^4 , and 1.01×10^4 s⁻¹ for **ICzTRZ**, **ICzTRZ-0**, **d⁴Bu-ICzTRZ** and **d⁴Bu-ICzTRZ**, respectively. The photoluminescence quantum yield (Φ_{PL}) for **ICzTRZ** has been measured as 84% under nitrogen and decreases to 73% in air, while the corresponding values of **d⁴Bu-ICzTRZ** are 81% and 70%, respectively. For the other two emitters, we do not have absolute PLQY data, but the relative intensities of their PL spectra are very similar to the first two, and since film thickness and host were identical, we conclude comparable PLQY values. This suggests that the incorporation of *tert*-butyl groups does not impact significantly the Φ_{PL} for this family series of emitters. The similar structures and PL spectra (singlet energies) of the four emitters explain why their decay kinetics are almost the same, although small differences mainly in their singlet energies do affect the triplet harvesting efficiency. We also note that the relatively high oscillator strength from the S₁ state (with CT character) to the ground state of about 0.7, and the only moderate RISC rates are consistent with the dihedral angles between donor and acceptor being far from orthogonal (about 50°), which is in contrast to TADF emitters like DMAC-TRZ, where this angle is close to 90°.

Orientation measurements

The orientation factor (θ) for these four emitter molecules was measured in several relevant host materials. The doped films (10 wt% emitter in the respective host matrix) were obtained *via* vacuum-deposition and the orientation of the emitter molecule was measured using angular dependant photoluminescence

spectroscopy (ADPL). Fig. 7 shows the obtained raw data for mCBP-CN as host, together with fits yielding θ at the respective peak emission wavelength. Table 5 collates the θ values for different hosts; measurement and fits are shown in the ESI† (Fig. S14–S16).

ICzTRZ presents a near complete horizontal orientation of its TDM regardless of the host material, with the strongest horizontal orientation found in DPEPO ($\theta = 0.06$), followed by mCBP-CN ($\theta = 0.07$), mCBP ($\theta = 0.09$), and the weakest alignment in mCP ($\theta = 0.12$). Overall, the TDM of **ICzTRZ** is the most horizontally aligned of the family of four emitters in this study.

For **ICzTRZ-0**, we find the highest θ values (*i.e.*, the least horizontal orientation of its TDM) of the four emitters. For **d⁴Bu-ICzTRZ-0** and **d⁴Bu-ICzTRZ**, we find very similar orientation parameters that are close to that of **ICzTRZ**. The presence of *tert*-butyl groups, regardless of location, has a positive effect with respect to the orientation factor (*i.e.*, leading to better horizontal orientation of the TDM, when compared to **ICzTRZ-0**, regardless of the nature of the host). This implies that a general increase in molecular weight, as opposed to the dimensionality or aspect ratio of the emitter, has the greatest influence on the θ value.

Organic light-emitting diodes

To demonstrate the impact of emitter orientation on device performance, we fabricated OLEDs with the four emitter materials and using mCBP-CN as the host. Patterned indium tin oxide (ITO) substrates were spin-coated with ~30 nm PEDOT:PSS along with 30 nm vacuum-deposited TCTA, which together act as the hole injection and transport side of the devices. This was followed by a 20 nm thick emission layer consisting of 10% emitter doped in mCBP-CN. We then deposited 40 nm TPBi along with 0.5 nm LiF and 100 nm aluminium on the electron transport side. LiF acts as a work function modifier for the aluminium cathode. The layer stack together with the obtained results are shown in Fig. 8.

Current–voltage–luminance characteristics (shown in the ESI,† Fig. S17) indicate that the devices need a relatively high

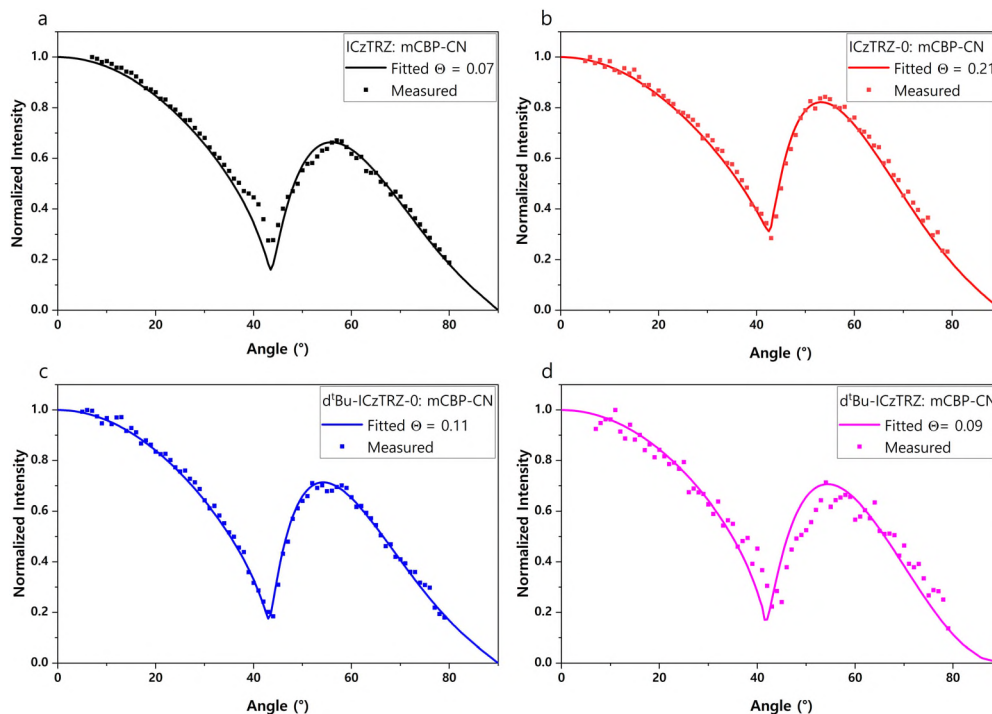


Fig. 7 Orientation measurements for 10 wt% emitters in mCBP-CN. Other host materials are shown in the ESI.† Excitation wavelength was 365 nm in all cases.

Table 5 Measured orientation values in different emitters in four matrices at 10 wt% doping concentration

θ	mCP	mCBP	mCBP-CN	DPEPO
ICzTRZ	0.12	0.09	0.07	0.06
ICzTRZ-0	0.18	0.17	0.21	0.15
d ⁴ Bu-ICzTRZ-0	0.11	0.09	0.11	0.09
d ⁴ Bu-ICzTRZ	0.10	0.10	0.09	0.09

voltage to turn on (~ 4 V), but they all achieve luminance values of about 5000 cd m^{-2} at 8 V. The relatively high drive voltages can be understood in view of the simple layer stack with significant injection barriers at both contacts. Nevertheless, the data can serve as a comparison for the performance of the four different emitter molecules. First, their electroluminescence spectra (shown in Fig. 8(b)) are in good agreement with the PL spectra discussed above. They exhibit the same FWHM trend and bathochromic shift of the emission peak wavelength from 498 nm for ICzTRZ & d⁴Bu-ICzTRZ along with 508 nm and 518 nm for ICzTRZ-0 and d⁴Bu-ICzTRZ-0 respectively. Their EQEs show an increase at low current densities with a maximum in the range $10\text{--}100 \text{ cd m}^{-2}$, before the EQE rolls-off at higher currents, most likely due to exciton quenching by charges or other biexcitonic pathways (Fig. 8(c)). The maximum EQE of the devices follows a similar trend as the orientation parameters of the emitters in mCBP-CN (Table 4), which confirms the link between device efficiency and the propensity for the emitter to have a horizontally aligned TDM, which affects the light outcoupling efficiency. The EQE values were measured over 8 devices in total with a distribution of values shown in Fig. 8(d).

Discussion

The focus of this work is to study structure–property relationships between the presence of *tert*-butyl substituents at different positions on the four different ICzTRZ-derivatives. The central goal was to manipulate the TDM orientation of these emitters in luminescent guest–host systems and investigate its effect on the photophysics and OLED efficiency of the related devices.

In general, molecular weight and T_g of both, emitter and host, are the main driving forces for emitter orientation. Comparing the different host materials, doped films in mCP ($T_g = 65 \text{ }^\circ\text{C}$, $M_w = 409 \text{ g mol}^{-1}$), which is the host molecule with the lowest T_g and M_w , are always (slightly) inferior to the doped films in mCBP-CN ($T_g = 113 \text{ }^\circ\text{C}$, $M_w = 510 \text{ g mol}^{-1}$) and DPEPO ($T_g = 93 \text{ }^\circ\text{C}$, $M_w = 571 \text{ g mol}^{-1}$). This confirms the established scaling of the orientation factor of emissive guest–host systems with the T_g of the host material.¹⁵

However, the comparison between the four emitters in a given host is not that straightforward to explain. Previous studies on emitter orientation have often used geometrical arguments, specifically the aspect ratio between the longest extension of an emitter molecule in one direction and the shortest one in a direction perpendicular to it³¹ or an aspect ratio that is based on the inertial moments tensor.^{32,33} But these simple predictors do not work here. For example, ICzTRZ-0 has the largest aspect ratio of 7.7 (derived from the inertial moments in Table 2) but the least horizontal orientation factor in all the hosts. And among the other emitters, there is also no clear correlation between this ratio and θ . Other authors have

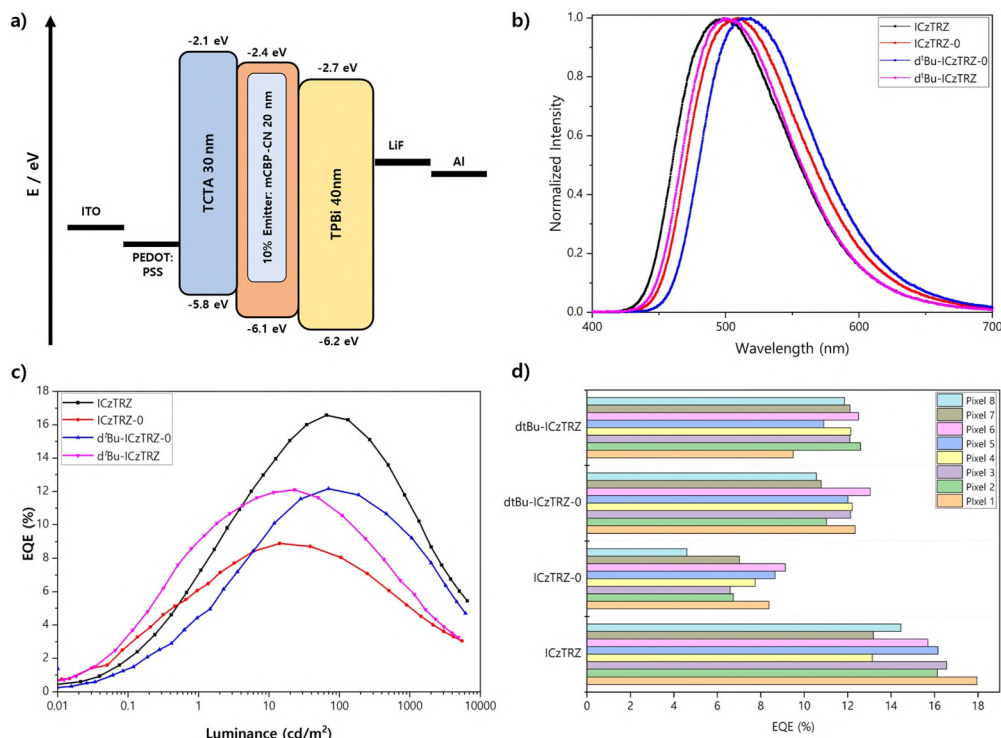


Fig. 8 OLED Devices. (a) Stack illustration, (b) EL spectrum, (c) Comparative EQE graph, (d) peak EQE distribution over different devices.

introduced slightly modified predictors for orientation,¹⁷ but also for these parameters (see Tables S5 and S6 of the ESI†) we do not find a clear correlation. As Tenopala *et al.* have suggested for emitters with high molecular weight (>600 g mol⁻¹), the primary predictor of orientation seems to be the emitter's M_w .¹⁷ **ICz-TRZ-0** (without any *tert*-butyl substituents) has the lowest MW of 871 g mol⁻¹ and, thus, the highest θ values. But for the other three emitter molecules (**d^tBu-ICzTRZ-0**: 983 g mol⁻¹, **ICzTRZ**: 1095 g mol⁻¹, and **d^tBu-ICzTRZ**: 1208 g mol⁻¹) the correlation is much weaker. They all have significantly lower θ values than **ICzTRZ-0**, but **ICzTRZ**, where the *tert*-butyl substituents are at the terminal acceptor positions, is the best. We think that for the subtle differences in molecular orientation between them, other factors like their electrostatic surface potentials might play a role as well, since the presence of *tert*-butyl substituents changes the ESP landscape as shown in Fig. 4. Specifically, the *tert*-butyl groups seem to have some shielding effect with their more or less neutral values, whereas the central ICz donor unit is strongly negative. Finally, regarding the “outlier” in orientation, **ICzTRZ-0**, one could even consider some influence of emitter aggregation due to the absence of any substituents, although we did not find direct evidence for it, *e.g.*, in the PL spectra for different emitter doping concentration.

Coming to the device data of the four emitters, we find that **ICzTRZ** has the best performance. But compared to our previous publication with the parent compound **ICzTRZ** as the emitter¹⁴ we find lower maximum device EQE, EQE_{max}, of 16% compared to 22%. This is mainly due to the simplified OLED stack used here without extra hole and electron blocking layers

that were present in the original report. As a consequence, the charge carrier balance is not ideal and there is a lack of carrier confinement for achieving close to unity recombination efficiency. Considering the relative variation of the peak EQEs between the four emitters, we have performed simulations of the light outcoupling factor based on their measured TDM orientations (see Fig. S18 and Table S8 of the ESI† for details). However, the predicted difference in this factor is relatively small (changing from about 35% for the most horizontal emitter **ICzTRZ** to slightly below 30% for the least horizontal emitter **ICzTRZ-0**). On the other hand, the Φ_{PL} of all four emitters is similar, at about 80% and also are their RISC efficiencies. This implies that the expected device EQEs should not differ by a factor of two between the best emitter (**ICzTRZ**) and the worst (**ICzTRZ-0**), as observed. Thus, we have to conclude, that there are additional electrical losses as well as exciton quenching, which reduce the EQE_{max} below the theoretically possible values. Moreover, the different shielding of the emitters as a result of the *tert*-butyl substituents seems not only to affect the TDM orientation but also the electronic properties of the materials as well as the electrical behaviour in the device. For example, it is known that more horizontal alignment of molecules in a thin-film device can improve its charge carrier mobility in the out-of-plane direction.¹⁴ And, also energy transfer from the host to the emitter molecules or direct charge trapping and recombination could be affected by the presence of *tert*-butyl substituents at different positions on the emitter molecules. But overall, we find a clear correlation between emitter orientation and OLED performance with **ICzTRZ** giving the highest EQEs and **ICzTRZ-0** the lowest values.

Conclusions

In this study, we report a family of structurally similar **ICzTRZ** derivatives containing different numbers and of *tert*-butyl substituents, positioned on either the triazine acceptor and/or the indolocarbazole donor. We correlated different structural parameters to the propensity for these emitters to align their TDMs horizontally in vacuum-deposited films. While **ICzTRZ-0**, which contains no *tert*-butyl substituents and is the lightest of the family of emitters, shows the largest orientation factor and hence has the least horizontally aligned TDM, **d^tBu-ICzTRZ** has only a slightly more horizontally aligned TDM, despite having the greatest number of *tert*-butyl groups. This is also the case for **d^tBu-ICzTRZ-0**. The compound with the most horizontally aligned TDM, irrespective of host, is **ICzTRZ**, which seems to have the best balance of its properties in terms of T_g , molecular weight, aspect ratio and ESP.

Author contributions

P. S. coordinated the writing of the manuscript, fabricated OLEDs and performed device measurements and simulations. E. C. performed DFT simulations and contributed to materials characterization. K. S. performed photophysical characterization. Z. Z. synthesized and characterized the materials. B. M. N. performed orientation measurements and part of the DFT simulations. D. W. performed thermal characterization. P. St., S. B. & A. P. M. coordinated and supervised the respective work in their labs. E. Z.-C. & W. B. conceived and coordinated the work. All authors contributed to the writing of the manuscript.

Data availability

The research data supporting this publication can be accessed at <https://doi.org/10.17630/ddbba299-9e48-4515-8f37-b8557b7113ae>. The data supporting this article have been included as part of the ESL.†

Conflicts of interest

The authors declare no conflict of interest.

Acknowledgements

The authors (P. S., E. C., K. S., M. B. N., P. St., A. P. M., E. Z.-C. & W. B.) would like to thank EU Horizon 2020 MSCA ITN TADFlife (grant agreement no. 812872) for financial support. Further support was provided by Deutsche Forschungsgemeinschaft (DFG) under project numbers 341263954, 449697195, and Germany's Excellence Strategy-3DMM2O-EXC-2082/1-390761711. E. Z.-C. thanks the Engineering and Physical Sciences Research Council (EP/W007517/1) for support.

References

- 1 H. Uoyama, K. Goushi, K. Shizu, H. Nomura and C. Adachi, Highly efficient organic light-emitting diodes from delayed fluorescence, *Nature*, 2012, **492**(7428), 234–238.
- 2 M. K. Etherington, J. Gibson, H. F. Higginbotham, T. J. Penfold and A. P. Monkman, Revealing the spin–vibronic coupling mechanism of thermally activated delayed fluorescence, *Nat. Commun.*, 2016, **7**(1), 13680.
- 3 J. Gibson, A. P. Monkman and T. J. Penfold, The importance of vibronic coupling for efficient reverse intersystem crossing in thermally activated delayed fluorescence molecules, *ChemPhysChem*, 2016, **17**(19), 2956–2961.
- 4 C. W. Tang, S. A. VanSlyke and C. H. Chen, Electroluminescence of doped organic thin films, *J. Appl. Phys.*, 1989, **65**(9), 3610–3616.
- 5 F. B. Dias, T. J. Penfold and A. P. Monkman, Photophysics of thermally activated delayed fluorescence molecules, *Methods Appl. Fluoresc.*, 2017, **5**(1), 012001.
- 6 B. Milián-Medina and J. Gierschner, Computational design of low singlet–triplet gap all-organic molecules for OLED application, *Org. Electron.*, 2012, **13**(6), 985–991.
- 7 T. D. Schmidt, T. Lampe, M. R. Sylvinson, P. I. Djurovich, M. E. Thompson and W. Brütting, Emitter Orientation as a Key Parameter in Organic Light-Emitting Diodes, *Phys. Rev. Appl.*, 2017, **8**(3), 037001.
- 8 D. Yokoyama, Molecular orientation in small-molecule organic light-emitting diodes, *J. Mater. Chem.*, 2011, **21**(48), 19187–19202.
- 9 J. Frischeisen, D. Yokoyama, C. Adachi and W. Brütting, Determination of molecular dipole orientation in doped fluorescent organic thin films by photoluminescence measurements, *Appl. Phys. Lett.*, 2010, **96**(7), 29.
- 10 A. Hofmann, M. Schmid and W. Brütting, The Many Facets of Molecular Orientation in Organic Optoelectronics, *Adv. Opt. Mater.*, 2021, **9**(21), 2101004.
- 11 S. S. Dalal, Z. Fakhraei and M. D. Ediger, High-throughput ellipsometric characterization of vapor-deposited indomethacin glasses, *J. Phys. Chem. B*, 2013, **117**(49), 15415–15425.
- 12 B. A. Naqvi, M. Schmid, E. Crovini, P. Sahay, T. Naujoks, F. Rodella, Z. Zhang, P. Stroehriegl, S. Bräse, E. Zysman-Colman and W. Brütting, What controls the orientation of TADF emitters?, *Front. Chem.*, 2020, **8**, 750.
- 13 C. Mayr and W. Brütting, Control of molecular dye orientation in organic luminescent films by the glass transition temperature of the host material, *Chem. Mater.*, 2015, **27**(8), 2759–2762.
- 14 D. Yokoyama, A. Sakaguchi, M. Suzuki and C. Adachi, Horizontal orientation of linear-shaped organic molecules having bulky substituents in neat and doped vacuum-deposited amorphous films, *Org. Electron.*, 2009, **10**(1), 127–137.
- 15 Z. Zhang, E. Crovini, P. L. dos Santos, B. A. Naqvi, D. B. Cordes, A. M. Z. Slawin, P. Sahay, W. Brütting, I. D. W. Samuel, S. Bräse and E. Zysman-Colman, Efficient Sky-Blue Organic Light-Emitting Diodes Using a Highly Horizontally Oriented Thermally Activated Delayed Fluorescence Emitter, *Adv. Opt. Mater.*, 2020, **8**(23), 2001354.

- 16 S. Xiang, X. Lv, S. Sun, Q. Zhang, Z. Huang, R. Guo, H. Gu, S. Liu and L. Wang, To improve the efficiency of thermally activated delayed fluorescence OLEDs by controlling the horizontal orientation through optimizing stereoscopic and linear structures of indolocarbazole isomers, *J. Mater. Chem. C*, 2018, **6**(21), 5812–5820.
- 17 F. Tenopala-Carmona, O. S. Lee, E. Crovini, A. M. Neferu, C. Murawski, Y. Olivier, E. Zysman-Colman and M. C. Gather, Identification of the Key Parameters for Horizontal Transition Dipole Orientation in Fluorescent and TADF Organic Light-Emitting Diodes, *Adv. Mater.*, 2021, **33**(37), 2100677.
- 18 S. Grimme, Density functional calculations with configuration interaction for the excited states of molecules, *Chem. Phys. Lett.*, 1996, **259**(1–2), 128–137.
- 19 T. Hosokai, H. Matsuzaki, H. Nakanotani, K. Tokumaru, T. Tsutsui, A. Furube, K. Nasu, H. Nomura, M. Yahiro and C. Adachi, Evidence and mechanism of efficient thermally activated delayed fluorescence promoted by delocalized excited states, *Sci. Adv.*, 2017, **3**(5), e1603282.
- 20 H. Noda, H. Nakanotani and C. Adachi, Excited state engineering for efficient reverse intersystem crossing, *Sci. Adv.*, 2018, **4**(6), eaao6910.
- 21 P. K. Samanta, D. Kim, V. Coropceanu and J.-L. Brédas, Up-conversion intersystem crossing rates in organic emitters for thermally activated delayed fluorescence: impact of the nature of singlet vs triplet excited states, *J. Am. Chem. Soc.*, 2017, **139**(11), 4042–4051.
- 22 P. L. Santos, J. S. Ward, P. Data, A. S. Batsanov, M. R. Bryce, F. B. Dias and A. P. Monkman, Engineering the singlet-triplet energy splitting in a TADF molecule, *J. Mater. Chem. C*, 2016, **4**(17), 3815–3824.
- 23 Y. Wada, H. Nakagawa, S. Matsumoto, Y. Wakisaka and H. Kaji, Organic light emitters exhibiting very fast reverse intersystem crossing, *Nat. Photonics*, 2020, **14**(10), 643–649.
- 24 M. Urban, P. H. Marek-Urban, K. Durka, S. Luliński, P. Pander and A. P. Monkman, TADF Invariant of Host Polarity and Ultralong Fluorescence Lifetimes in a Donor–Acceptor Emitter Featuring a Hybrid Sulfone-Triarylboron Acceptor, *Angew. Chem., Int. Ed.*, 2023, **62**(9), e202217530.
- 25 A. D. Bochevarov, E. Harder, T. F. Huges, J. R. Greenwood, D. A. Brandon, D. M. Philipp, D. Rinaldo, M. D. Halls, J. Zhang and R. A. Friesner., Jaguar: A high-performance quantum chemistry software program with strengths in life and materials sciences, *Int. J. Quantum Chem.*, 2013, 2110–2142.
- 26 K. Stavrou, L. G. Franca and A. P. Monkman, Photophysics of TADF Guest-Host Systems: Introducing the Idea of Hosting Potential, *ACS Appl. Electron. Mater.*, 2020, **2**(9), 2868–2881.
- 27 K. H. Kim and J. J. Kim, Origin and control of orientation of phosphorescent and TADF dyes for high-efficiency OLEDs, *Adv. Mater.*, 2018, **30**(42), 1705600.
- 28 D. Zhang, X. Song, M. Cai, H. Kaji and L. Duan, Versatile indolocarbazole-isomer derivatives as highly emissive emitters and ideal hosts for thermally activated delayed fluorescent OLEDs with alleviated efficiency roll-off, *Adv. Mater.*, 2018, **30**(7), 1705406.
- 29 M. Jian, Z. Song, X. Chen, J. Zhao, B. Xu and Z. Chi, Afterglows from the indolocarbazole families, *Chem. Eng. J.*, 2022, **429**, 132346.
- 30 M. Mahmoudi, E. Urbonas, D. Volyniuk, D. Gudeika, K. Dabrovskas, J. Simokaitiene, A. Dabulienė, R. Keruckienė, K. Leitonas and M. Guzauskas, Indolocarbazoles with Sterically Unrestricted Electron-Accepting Anchors Showcasing Aggregation-Induced Thermally Activated Delayed Mechanoluminescence for Host-Free Organic Light-Emitting Diodes, *Molecules*, 2023, **28**(16), 5999.
- 31 M. Schmid, K. Harms, C. Degitz, T. Morgenstern, A. Hofmann, P. Friederich, H.-H. Johannes, W. Wenzel, W. Kowalsky and W. Brütting, Optical and electrical measurements reveal the orientation mechanism of homoleptic iridium-carbene complexes, *ACS Appl. Mater. Interfaces*, 2020, **12**(46), 51709–51718.
- 32 M. C. Jung, J. Facendola, J. Kim, D. S. Muthiah Ravinson, P. I. Djurovich, S. R. Forrest and M. E. Thompson, Molecular Alignment of Homoleptic Iridium Phosphors in Organic Light-Emitting Diodes, *Adv. Mater.*, 2021, **33**(36), 2102882.
- 33 B. M. Nguyen, M. Schmid, J. Kirsch, A. Cakaj and W. Brütting, On the Orientation Mechanism of Nonpolar Dyes in Light-Emitting Guest–Host Systems, *Chem. Mater.*, 2023, **35**(17), 7333–7343.